0026-895X/06/7001-405–414$20.00
MOLECULAR PHARMACOLOGY
Copyright © 2006 The American Society for Pharmacology and Experimental Therapeutics
Mol Pharmacol 70:405–414, 2006

Vol. 70, No. 1
22970/3124707
Printed in U.S.A.

Potent Modulation of the Voltage-Gated Sodium Channel $Na_v1.7$ by OD1, a Toxin from the Scorpion *Odonthobuthus doriae*

Chantal Maertens, Eva Cuypers, Mehriar Amininasab, Amir Jalali, Hossein Vatanpour, and Jan Tytgat

Laboratory of Toxicology, University of Leuven, Leuven, Belgium (C.M., E.C., J.T.); Department of Cell and Molecular Biology, Faculty of Science, University of Tehran, Tehran, Iran (M.A.); Department of Toxicology and Pharmacology, Jundishapour University of Medical Sciences, Ahvaz, Iran (A.J.); and Department of Toxicology and Pharmacology, Shaheed Beheshti University of Medical Science, Tehran, Iran (H.V.)

Received January 26, 2006; accepted April 26, 2006

ABSTRACT

Voltage-gated sodium channels are essential for the propagation of action potentials in nociceptive neurons. $Na_v1.7$ is found in peripheral sensory and sympathetic neurons and involved in short-term and inflammatory pain. $Na_v1.8$ and $Na_v1.3$ are major players in nociception and neuropathic pain, respectively. In our effort to identify isoform-specific and high-affinity ligands for these channels, we investigated the effects of OD1, a scorpion toxin isolated from the venom of the scorpion *Odonthobuthus doriae.* $Na_v1.3$, $Na_v1.7$, and $Na_v1.8$ channels were coexpressed with β_1-subunits in *Xenopus laevis* oocytes. Na^+ currents were recorded with the two-electrode voltage-clamp technique. OD1 modulates $Na_v1.7$ at low nanomolar concentrations: 1) fast inactivation is dramatically impaired, with an EC_{50} value of 4.5 nM; 2) OD1 substantially increases the peak current at all voltages; and 3) OD1 induces a substantial persistent current. $Na_v1.8$ was not affected by concentrations up to 2 μM, whereas $Na_v1.3$ was sensitive only to concentrations higher than 100 nM. OD1 impairs the inactivation process of $Na_v1.3$ with an EC_{50} value of 1127 nM. Finally, the effects of OD1 were compared with a classic α-toxin, AahII from *Androctonus australis* Hector and a classic α-like toxin, BmK M1 from *Buthus martensii* Karsch. At a concentration of 50 nM, both toxins affected $Na_v1.7$. $Na_v1.3$ was sensitive to AahII but not to BmK M1, whereas $Na_v1.8$ was affected by neither toxin. In conclusion, the present study shows that the scorpion toxin OD1 is a potent modulator of $Na_v1.7$, with a unique selectivity pattern.

Voltage-gated sodium channels (VGSC) are the signature channels of excitable cells. The channels are large and complex proteins that open transiently upon membrane depolarization, giving the upstroke of the action potential. They consist of a pore forming α-subunit and auxiliary β-subunits. So far, 10 mammalian α-subunits ($Na_v1.1$–$Na_v1.9$, Na_x) and four β-subunits have been cloned. The β-subunits modulate the localization, expression, and functional properties of α-subunits (Catterall et al., 2005). Different α-subunits have distinct electrophysiological and pharmacological properties, and they are targeted by a large variety of chemically different toxins from animal venoms and plants (Wang and Wang, 2003). Many loss-of-function and gain-of-function mutations of α-subunits have been identified in human conditions characterized with epilepsy, seizures, ataxia, and increased sensitivity to pain (Meisler and Kearney, 2005).

Physiological and pharmacological evidence has demonstrated a critical role for VGSCs in many types of pain syndromes (Wood et al., 2004). Two VGSCs, $Na_v1.8$ and $Na_v1.9$, are expressed selectively in damage-sensing peripheral neurons, whereas a third channel, $Na_v1.7$, is found predominantly in sensory and sympathetic neurons and is implicated in inflammatory pain. An embryonic channel, $Na_v1.3$, is also up-regulated in damaged peripheral nerves and associated with increased electrical excitability in neuropathic pain states. A combination of antisense and knock-out studies support a specialized role for these VGSCs in pain pathways, and pharmacological studies with some peptidyl toxins suggest that isoform-specific antagonists should be feasible and therefore could be useful analgesics (Wood et al., 2004).

In addition to its role in inflammatory pain (Nassar et al.,

C.M. is a postdoctoral fellow of the Fonds voor Wetenschappelijk onderzoek-Vlaanderen (FWO-Vlaanderen). This work was supported by grants G.0330.06 from FWO-Vlaanderen and OT-05-64 from Katholieke Universiteit Leuven.

Article, publication date, and citation information can be found at http://molpharm.aspetjournals.org.

doi:10.1124/mol.106.022970.

ABBREVIATIONS: VGSC, voltage-gated sodium channel; AUC, area under the current-voltage curve; I-V, current-voltage.

2004; Yeomans et al., 2005), $Na_v1.7$ has been implicated in other pathophysiological conditions. Recent work has shown that autosomal dominant erythermalgia is associated with mutations in this VGSC (Dib-Hajj et al., 2005; Drenth et al., 2005; Michiels et al., 2005; Waxman and Dib-Hajj, 2005). Furthermore, functional expression of $Na_v1.7$ has been linked with strong metastatic potential in prostate cancer, and this channel has been suggested to be a functional diagnostic marker (Diss et al., 2005).

Despite its clinical importance, the pharmacological characterization of $Na_v1.7$ is not very elaborate, and a selective high-affinity modulator is still missing. The local anesthetic and class I antiarrhythmic lidocaine, a well known VGSC modulator, decreases $Na_v1.7$ currents in a frequency-dependent matter, with an EC_{50} value of 450 μM (Chevrier et al., 2004). In addition, recent work showed that the T-type Ca^{2+} channel antagonist mibefradil is a state-dependent VGSC modulator, blocking $Na_v1.2$, $Na_v1.4$, $Na_v1.5$, and $Na_v1.7$ at low micromolar concentrations (McNulty and Hanck, 2004). Two tarantula peptides, ProTx-I and ProTx-II, isolated from *Thrixopelma pruriens*, inhibit activation of $Na_v1.2$, $Na_v1.5$, $Na_v1.7$, and $Na_v1.8$ in the nanomolar range (Middleton et al., 2002). Heinemann and coworkers demonstrated that the scorpion α-toxins Lqh-2 and Lqh-3 from *Leiurus quinquestriatus hebraeus*, previously described as potent modulators of $Na_v1.5$ (Chen and Heinemann, 2001) and $Na_v1.4$ (Chen et al., 2000), impair the inactivation process of $Na_v1.7$ at low nanomolar concentrations (Chen et al., 2002).

In the field of scorpion toxinology, the Asian scorpion *Buthus martensii* Karsch has received notable attention with reference to pain. A number of analgesic peptides from its venom have been reported; for most of them, it can be assumed that they could target VGSCs by virtue of their primary structure homology and similar scaffold with so-called long-chain sodium channel toxins (Goudet et al., 2002). They are: BmK ITAP, an excitatory insect-selective toxin (Xiong et al., 1999); BmK dITAP3, a depressant insect-selective toxin (Guan et al., 2001a) with an analgesic effect in mice; BmK AGAP, an antitumor analgesic peptide showing inhibitory effect on both visceral and somatic pain (Liu et al., 2003); BmK Ang P1 (Guan et al., 2001b); BmK AngM1 (Cao et al., 2004); BmK AS (Chen and Ji, 2002); BmK IT2 (Wang et al., 2000); BmK I1; BmK I4; and BmK I6 (Guan et al., 2000). All of these are peptides for which analgesic properties in mice have been demonstrated. These findings indicate that scorpion toxins can be a valuable source of potential analgesics.

In the present study, we investigated the effect of the recently discovered scorpion toxin OD1 (Fig. 1), on three VGSCs implicated in pain sensation (i.e., $Na_v1.3$, $Na_v1.7$, and $Na_v1.8$). Most scorpion neurotoxins targeting VGSCs are single-chain polypeptides composed of 60 to 70 amino acids cross-linked by 4-disulfide bridges. They comprise two main groups: α- and β-toxins (Possani et al., 1999). Scorpion α-toxins bind to site 3 and slow down the inactivation process. According to their different pharmacological and binding properties, the α-toxins can be further divided into three subgroups: classic α-toxins, α-like toxins, and insect α-toxins. Classic α-toxins (e.g., AahII, Lqh-2) are highly toxic to mammals, whereas the insect α-toxins (e.g., LqhαIT) are highly toxic to insects. The α-like toxins (e.g., Lqh-3, BmK M1) act on both mammals and insects (Gordon et al., 1996; Goudet et al., 2002; Rodriguez de la Vega and Possani, 2005). OD1 is the first toxin isolated from the Iranian yellow scorpion *Odonthobuthus doriae* and was recently characterized as an α-like toxin. Jalali et al. (2005) showed that the inactivation process of the insect channel, para/tipE, was severely hampered by 200 nM OD1 (EC_{50} = 80 ± 14 nM), whereas $Na_v1.2/\beta_1$ still was not affected at concentrations up to 5 μM. $Na_v1.5/\beta_1$ was influenced only at micromolar concentrations (Jalali et al., 2005).

Materials and Methods

Sodium Channel Expression in *Xenopus laevis* Oocytes. For in vitro transcription, rβ_1/pSP64T was first linearized with EcoRI. Next, capped cRNAs were synthesized from the linearized plasmid using the large-scale SP6 mMESSAGE mMACHINE transcription kit (Ambion, Austin, TX). The hNav1.8/pBSTA, rNav1.7/pBSTA, rNav1.3/pNa3T, and hβ_1/pGEM-HE vectors were linearized with NotI, SacII, NotI, and NheI, respectively, and transcribed with the T7 mMESSAGE-mMACHINE kit.

The harvesting of oocytes from anesthetized female *X. laevis* frogs was performed as described previously (Tytgat et al., 1997). Oocytes were injected with 50 nl of cRNA at a concentration of 1 ng/nl using a microinjector (Drummond Scientific, Broomall, PA). The solution used for incubating the oocytes (ND-96 solution) contained 96 mM NaCl, 2 mM KCl, 1.8 mM $CaCl_2$, 2 mM $MgCl_2$, and 5 mM HEPES, pH 7.4, supplemented with 50 mg/l gentamicin sulfate and 180 mg/l theophylline (except for $Na_v1.7$).

Electrophysiological Measurements. Sodium currents were recorded using the *X. laevis* expression system. Two-electrode voltage-clamp recordings were performed at room temperature (18–22°C) using a GeneClamp 500 amplifier controlled by a pClamp data acquisition system (Molecular Devices, Sunnyvale, CA). Whole-cell currents from oocytes were recorded 2 to 4 days after injection. Current and voltage electrodes had resistances as low as possible (0.2–1 MΩ) and were filled with 3 M KCl. Currents were sampled at 5 kHz and filtered at 1 kHz using a four-pole low-pass Bessel filter. Leak subtraction was performed using a −P/4 protocol. To eliminate the effect of the voltage drop across the bath-grounding electrode, the bath potential was actively controlled. Voltage records were carefully monitored on an oscilloscope (HAMEG Instruments GmbH, Mainhausen, Germany).

The bath solution was ND-96 solution. Toxins were added directly to the recording chamber from a stock solution in ND-96 to obtain the desired final concentration. Immediately after adding the toxin stock solution at some distance from the oocyte, the bath solution was mixed to obtain a homogenous final concentration within a few seconds.

For activation protocols, 100-ms test depolarizations ranging from −45 to +70 mV were applied from a holding potential of −100 mV in

```
OD1       GVRDAYIADDKNCVYTCAS-NGYCNTECTKNGAESGYCQWIGRYGNACWCIKLPDEVPIRIPG-KCR      100 %

BmK M1    -VRDAYIAKPHNCVYECAR-NEYCNDLCTKNGAKSGYCQWVGKYGNGCWCIELPDNVPIRVPG-KCH       75 %
AaH II    -VKDGYIVDDVNCTYFCGR-NAYCNEECTKLKGESGYCQWASPYGNACYCYKLPDHVRTKGPG-RCN       60 %
Lqh-2     -IKDGYIVDDVNCTYFCGR-NAYCNEECTKLKGESGYCQWASPYGNACYCYKLPDHVRTKGPG-RCR       60 %
Lqh-3     -VRDGYIAQPENCVYHCFPGSSGCDTLCKEKGGTSGHCGFKVGHGLACWCNALPDNVGIIVDGVKCH       44 %
```

Fig. 1. Comparison of amino acid sequence of OD1 with BmK M1, AahII, Lqh-2 and Lqh-3. Alignment is based on cystine residues (indicated in bold) using ClustalW (http://www.ebi.ac.uk/clustalw/). Percentage similarity is shown relative to OD1.

5-mV increments, at an interval of 5 s. Voltage-dependent steady-state inactivation was determined by means of a double-pulse protocol in which a conditioning pulse was applied from a holding potential of −100 mV to a range of potentials from −90 (or −70) mV to 0 (or −5) mV in 5-mV increments for 50 ms, immediately followed by a test pulse to 0 (or −5) mV. The peak current amplitudes during the tests were normalized to the amplitude of the first pulse and plotted against the potential of the conditioning pulse. The voltage dependence of the relative current (activation and fast inactivation) was fit by a Boltzmann function. Recovery from fast inactivation was examined using a standard double-pulse protocol. A 25-ms conditioning pulse to 0 mV was used to fully fast-inactivate the channel. The membrane was then hyperpolarized to −100 mV from 0 to 160 ms, and the recovery was monitored by measuring the relative peak Na^+ current elicited by a second pulse to 0 mV. The interval between the pulses was 5 s. The recovery of the peak amplitude was fitted with a double exponential. Data were analyzed in Winascd (Guy Droogmans, Katholieke Universiteit, Leuven, Belgium) and in Origin (OriginLab Corp., Northampton, MA).

Quantification of Toxin Effects. To assay the complex effects of the toxin, two parameters were determined: 1) the increased influx of Na^+ ions at different voltages was quantified by measuring the area under the current-voltage (I-V) curve (AUC) in control conditions and in the presence of the toxin, and 2) the degree of fast inactivation was assayed by measuring the peak current as well as the current amplitude at 30 ms after the start of the depolarization. The ratio I_{30ms}/I_{peak} gives an estimate for the fast inactivation process and similar parameters have been used by others as a measure of fast inactivation (Chen et al., 2002).

The dose dependence for toxin-induced effects was measured by plotting the parameter I_{30ms}/I_{peak} as a function of toxin concentration. The concentration dependence was described with the following dose-response equation: effect $= A_1 + \{A_2 - A_1/[1 + (EC_{50}/[\text{toxin}])^{n_H}]\}$, where n_H is the Hill coefficient, [toxin] is the toxin concentration, and EC_{50} is the concentration of half-maximal effect. A_1 is the offset and was determined from experiments in the absence of toxin ([toxin] = 0). For fitting the data, the A_1 value was fixed to the value obtained under control conditions. The value A_2 is measured for the maximal effect of the toxin and was determined from the fits.

Results

Differential Effects of OD1 on $Na_v1.7$, $Na_v1.3$, and $Na_v1.8$. Figure 2 shows representative whole-cell Na^+ currents recorded from oocytes expressing $Na_v1.7$, $Na_v1.3$, and

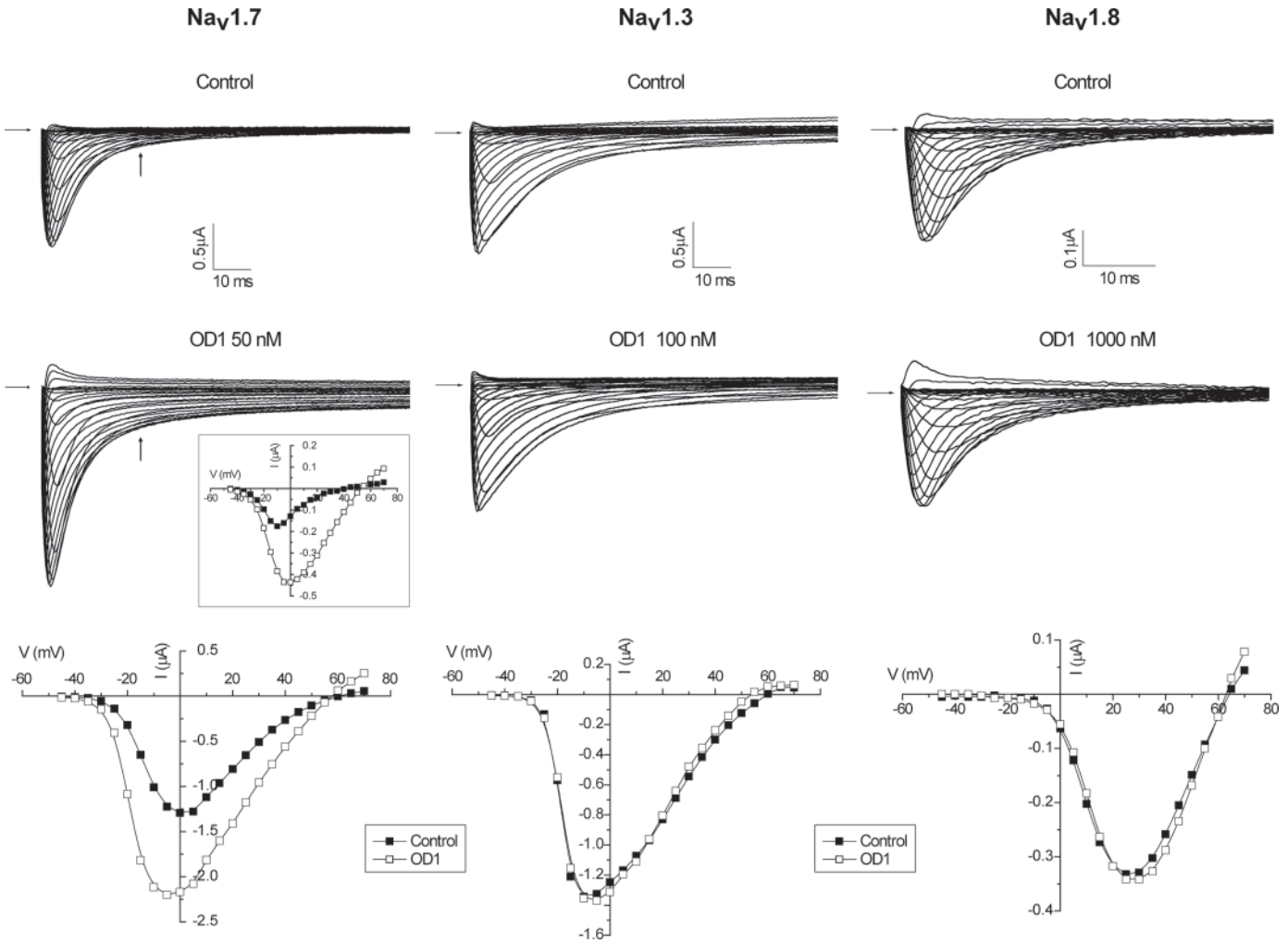

Fig. 2. Differential effects of OD1 on $Na_v1.7$, $Na_v1.3$, and $Na_v1.8$ Na^+ channels heterologously expressed in *X. laevis* oocytes. Representative whole cell Na^+ currents of oocytes expressing $Na_v1.7$ (left), $Na_v1.3$ (middle), and $Na_v1.8$ (right) in control conditions and in the presence of different concentrations of OD1. Horizontal arrows indicates zero current. Currents were elicited by depolarizing steps between −45 and +70 mV in 5-mV increments from a holding potential of −100 mV. Corresponding current-voltage relationship for control conditions (■) and in the presence of OD1 (□) are depicted at the bottom of the figure. Vertical arrows ($Na_v1.7$) indicate time at 30 ms. Inset, corresponding current-voltage relation at that certain point in time.

$Na_v1.8$ in control conditions (top) and in the presence of 50 nM ($Na_v1.7$), 100 nM ($Na_v1.3$), and 1000 nM ($Na_v1.8$) OD1 (middle). Na^+ currents were evoked by applying a series of depolarizing voltage steps between −45 and +70 mV in 5-mV increments. The bottom shows the corresponding I-V curves in control conditions (■) and in the presence of OD1 (□).

Compared with control conditions, 50 nM OD1 has dramatic effects on $Na_v1.7$ currents: 1) the inactivation is impaired, 2) there is a substantial persistent current at the end of the 100-ms voltage step, and 3) there is an increase in inward peak current. This last effect is visible at all voltages and was quantified by measuring the AUC. OD1 (50 nM) increases the AUC with 170 ± 10% (n = 4). The impairment of the inactivation process becomes clear by comparing the current amplitude at 30 ms (vertical arrow) for control conditions and in the presence of 50 nM OD1. The inset shows the corresponding I_{30ms}-voltage relation. At 50 nM OD1, $Na_v1.3$ and $Na_v1.8$ were not affected. $Na_v1.8$ is completely insensitive to 1000 nM OD1, whereas $Na_v1.3$ was unaffected by concentrations up to 100 nM.

$Na_v1.3$ is affected by higher concentrations of OD1. The modulation of $Na_v1.3$ by 500 nM OD1 is less dramatic but similar to the effects of 50 nM OD1 to $Na_v1.7$: there is an increase in peak current, a larger persistent current at the end of the test pulse and an impairment of the fast inactivation process.

We used this last parameter to quantify and compare the effects of OD1 on these two VGSCs. Figure 3 shows the relative I_{30ms}/I_{peak} in function of increasing concentrations of OD1 for $Na_v1.7$ (squares) and $Na_v1.3$ (circles). Each data point represents the mean ± S.E.M. (n = 3–6). The dotted line represents the best fit of the data to the dose-response equation described above. The EC_{50} value and Hill coefficient were 4.5 ± 0.2 nM and 1.5 ± 0.1, respectively, for $Na_v1.7$ and 1127 ± 263 nM and 1.1 ± 0.2, respectively, for $Na_v1.3$. These values demonstrate that OD1 displays a selectivity for $Na_v1.7$.

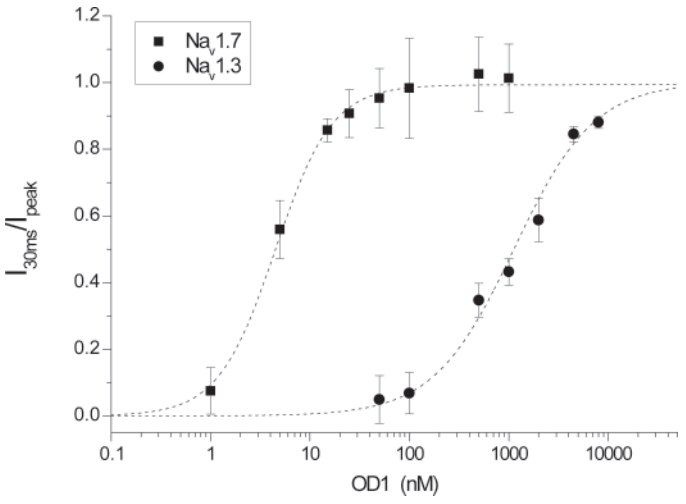

Fig. 3. $Na_v1.7$ and $Na_v1.3$ have different sensitivities to OD1. Dose-response curves for OD1 on $Na_v1.7$ (■) and $Na_v1.3$ (●) channels obtained by plotting the relative I_{30ms}/I_{peak} values in function of the toxin concentrations, fitted with the dose-response equation under *Quantification of Toxin Effects* yielding an EC_{50} value and Hill coefficient. For $Na_v1.7$, these values were 4.5 ± 0.2 nM and 1.5 ± 0.1, respectively. For $Na_v1.3$, they were 1127 ± 263 nM and 1.1 ± 0.2, respectively. Each data point is an average from three to six experiments.

Effects of OD1 on the Gating of $Na_v1.7$ and $Na_v1.3$. The availability of Na^+ channels upon depolarization is dependent on the cell membrane resting potential. Fewer channels become available as the resting membrane potential progressively moves toward more depolarized voltages. This effect is due to the accumulation of channels in the nonconducting inactivated state. This phenomenon was measured experimentally using constant conditioning pulses to voltages between −90 and 0 mV. The fraction of available current left was measured by standard test pulses (0 mV for $Na_v1.7$ and −5 mV for $Na_v1.3$). The normalized currents were then plotted against the conditioning voltage in the absence and presence of OD1 (Fig. 4, top, $Na_v1.7$; bottom, $Na_v1.3$). OD1 (50 nM) does not significantly shift the $V_{1/2}$ of

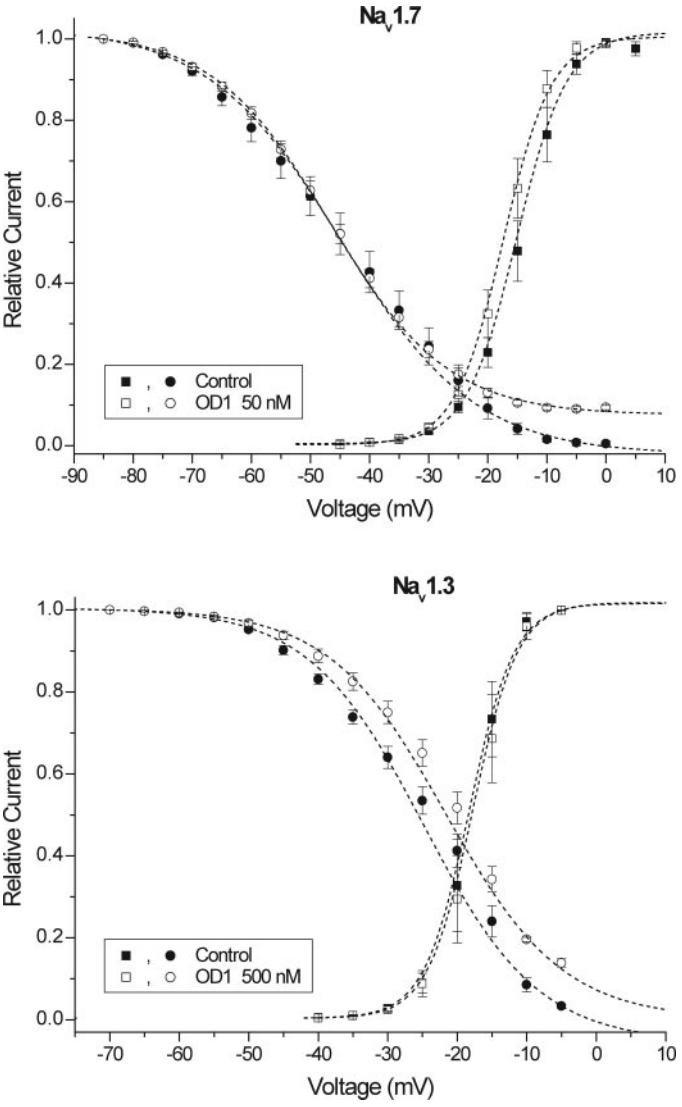

Fig. 4. Effect of OD1 on the activation and steady-state inactivation curves of $Na_v1.7$ (top) and $Na_v1.3$ (bottom). Activation curves (squares) were derived from the same family of currents used for the current-voltage curves (Fig. 2) using the standard procedure (see *Materials and Methods*). Steady-state inactivation curves (circles) were determined using conditioning pulses to voltages between −90 and 0 mV and a standard test pulse to 0 mV for $Na_v1.7$ or −5 mV for $Na_v1.3$. Test currents were normalized and plotted against the conditioning voltage. The steady-state properties for $Na_v1.7$ and $Na_v1.3$ in the absence of OD1 (■, ●) are shown on the same graph as in the presence of OD1 (□, ○). Each data point is an average of at least three experiments. The dashed lines are Boltzmann fits. See Table 1 for $V_{1/2}$ values and slope factors.

inactivation for $Na_v1.7$ ($p < 0.05$) (Table 1). However, OD1 has clear effects on the completeness of the inactivation. At 0 mV, the availability was 0.53 ± 0.65% in control conditions but 9.4 ± 0.5% in the presence of 50 nM OD1. For $Na_v1.3$, 500 nM OD1 induced a nonsignificant small depolarizing shift of 3 mV in the $V_{1/2}$ of inactivation ($p < 0.05$). $V_{1/2}$ and slope factors are depicted in Table 1. As for $Na_v1.7$, the inactivation of $Na_v1.3$ in the presence of OD1 is less complete. The percentage of available channels at −5 mV was 3.3 ± 0.5% in control conditions and 13.9 ± 1% in the presence of 500 nM OD1.

The effect of OD1 on the activation of the two channels was also investigated. The activation curves were derived from the I-V curves. The activation curves of $Na_v1.7$ and $Na_v1.3$ in the absence and presence of OD1 were plotted against voltage (Fig. 4, top, $Na_v1.7$; bottom, $Na_v1.3$). For $Na_v1.7$, 50 nM OD1 caused a 3-mV hyperpolarizing shift of the midpoint of activation. This shift was not significant ($p < 0.05$, Table 1), but became larger with higher concentrations of OD1 (data not shown). For $Na_v1.3$, 500 nM OD1 did not affect the activation process (Table 1).

Effect of OD1 On the Recovery from Fast Inactivation of $Na_v1.7$. Next, we examined the recovery from fast inactivation in the absence and presence of OD1. Figure 5 shows the fraction of recovered $Na_v1.7$ channels for control conditions and in the presence of 100 nM OD1 (mean ± S.E.M., $n = 3$). The two time constants (see inset) are 8.8 ± 0.2 and 46.8 ± 5.3 ms for the control condition and 1.8 ± 0.2 and 11.8 ± 0.3 ms in the presence of OD1, indicating that OD1 accelerates the recovery from fast inactivation of $Na_v1.7$.

Comparison of OD1 Effects with AahII and BmK M1. To investigate whether the multiple effects were typical for OD1, we compared OD1 with a classic α-toxin, AahII from *Androctonus australis* Hector (Rochat et al., 1972), and a classic α-like toxin, BmK M1 from *B. martensii* Karsch (Ji et al., 1996) (Fig. 1). Figure 6, A and D, shows $Na_v1.7$ current traces in response to a 100-ms voltage step to 0 mV in control conditions and in the presence of 50 nM AahII or 50 nM BmK M1. Like OD1, both AahII and BmK M1 induce 1) an increase in peak current, 2) an impairment of the inactivation process, and 3) a large persistent current at the end of 100-ms voltage step, indicating that these three effects are not unique to OD1. The absolute values of the parameter I_{30ms}/I_{peak} were 0.17 ± 0.01 for 50 nM OD1, 0.18 ± 0.02 for 50 nM AahII, and 0.12 ± 0.01 for 50 nM BmK M1. Those values represent the mean ± S.E.M. of at least three experiments. For comparison, under control conditions, this value was 0.048 ± 0.009 ($n = 9$), implying that the ratio I_{30ms}/I_{peak} increases 3.6-fold for 50 nM OD1, 3.8-fold for 50 nM AahII, and 2.5-fold for 50 nM BmK M1. Figure 6, B and E, shows the corresponding current-voltage relation recorded from the same oocyte as in Fig. 6, A and D, respectively. At a concentration of 50 nM, both toxins substantially increase the area under the I-V curve. For this representative example, the increase in the AUC was 200% for AahII and 160% for BmK M1.

The effects of 50 nM AahII and BmK M1 on the gating of $Na_v1.7$ are represented in the bottom of Fig. 6, C and F. Tables 2 (AahII) and 3 (BmK M1) show the corresponding $V_{1/2}$ values and slope factors, as determined by fitting the data points to the Boltzman equation. The activation process of $Na_v1.7$ is not affected by 50 nM AahII or BmK M1, whereas the steady-state inactivation is modified only by AahII. The latter causes a significant ($p < 0.05$) depolarizing shift of 5.3 mV in the $V_{1/2}$. Similar to OD1, both toxins reduce the completeness of steady-state inactivation. The percentage of available channels at −5 mV was 14.5 ± 3.4% in the presence of 50 nM AahII and 9.7 ± 0.4% the presence of 50 nM BmK M1.

In addition, we also investigated the effects of 50 nM AahII and BmK M1 on $Na_v1.3$ and $Na_v1.8$. At this concentration, $Na_v1.8$ was affected by neither AahII ($n \geq 5$) nor BmK M1 ($n \geq 4$). In addition, concentrations up to 500 nM were tested

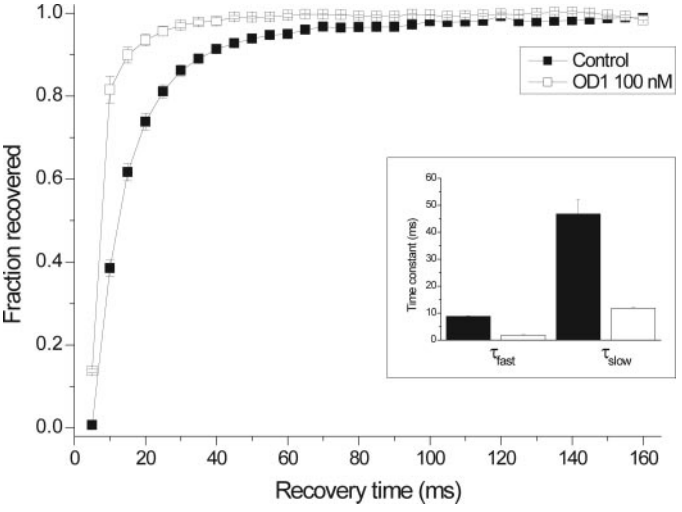

Fig. 5. Effect of OD1 on the recovery of fast inactivation of $Na_v1.7$. Recovery from fast inactivation examined using a standard double-pulse protocol. A 25-ms conditioning pulse to 0 mV to fully fast-inactivate the channel, followed by a hyperpolarizing step to −100 mV for variable duration (0–160 ms). Recovery was monitored by measuring the relative peak Na^+ current elicited by a second pulse to 0 mV and plotted as a function of the interval between the pulses. The average of at least three experiments is depicted for control conditions (■) and in the presence of 100 nM OD1 (□). The recovery of the peak amplitude was fitted with a double exponential. The inset shows the time constants for control conditions (filled bar) and in the presence of 100 nM OD1 (open bar).

TABLE 1
Effects of OD1 on fast activation and inactivation parameters for $Na_v1.7$ and $Na_v1.3$

	Activation			Inactivation		
	$V_{1/2}$	Slope	n	$V_{1/2}$	Slope	n
	mV			*mV*		
$Na_v1.7$						
Control	−15.1 ± 0.5	4.2 ± 0.2	4	−44.8 ± 0.7	11.3 ± 0.4	4
OD1 50 nM	−17.4 ± 0.4	4.1 ± 0.2	4	−46.7 ± 0.4	10.0 ± 0.3	4
$Na_v1.3$						
Control	−18.3 ± 0.6	3.2 ± 0.1	3	−24.8 ± 1.1	8.3 ± 0.4	3
OD1 500 nM	−17.8 ± 0.5	3.2 ± 0.2	3	−21.6 ± 0.9	8.4 ± 0.3	3

and induced no change in $Na_v1.8$ currents. $Na_v1.3$ however is sensitive to 50 nM AahII. Figure 7A shows $Na_v1.3$ current traces in response to a 100-ms voltage step to −5 mV in control conditions and in the presence of 50 nM AahII. AahII induces 1) an increase in peak current, 2) an impairment of the inactivation process, and 3) a large persistent current at the end of a 100-ms voltage step. The absolute values of the parameter I_{30ms}/I_{peak} were 0.23 ± 0.02 in control and 0.70 ± 0.01 in the presence of 50 nM AahII ($n \geq 4$), resulting in a 3.1-fold increase of the I_{30ms}/I_{peak} ratio. Figure 7B shows the corresponding current-voltage relation recorded from the same oocyte. At a concentration of 50 nM, AahII increases the AUC with 240%. The effects on the activation and steady-state inactivation curves of $Na_v1.3$ is depicted in Fig. 6C. The corresponding $V_{1/2}$ values and slope factors, as determined by fitting the data points to the Boltzman equation, are shown in Table 2. AahII (50 nM) causes a 8.7-mV hyperpolarizing shift in the $V_{1/2}$ for activation. The $V_{1/2}$ for steady-state inactivation was not affected, but the completeness of steady-state inactivation changed dramatically in the presence of 50 nM AahII. The percentage of available channels at −5 mV increased from 3.7 ± 0.5% in control conditions to 53.9 ± 2.9% in the presence of 50 nM AahII.

$Na_v1.3$ was not sensitive to 50 nM BmK M1. Figure 7D shows $Na_v1.3$ current traces in response to a 100-ms voltage step to −5 mV in control conditions and in the presence of 50 nM BmK M1. Figure 7E shows the current-voltage curve recorded from the same oocyte, demonstrating that BmK M1 does not affect this channel. Higher concentrations (up to 500 nM) did not induce significant changes in $Na_v1.3$ currents (data not shown). The activation and steady-state inactivation curves are depicted in Fig. 7F. The corresponding $V_{1/2}$ values and slope factors, as determined by fitting the data points to the Boltzman equation, are shown in Table 3. BmK M1 at a concentration of 50 nM induced no significant ($p < 0.05$) in the activation or inactivation parameters.

Discussion

The aim of this study was to examine the effects of the recently discovered scorpion toxin OD1 (Fig. 1), on three VGSCs involved in pain sensation: $Na_v1.3$, $Na_v1.7$, and

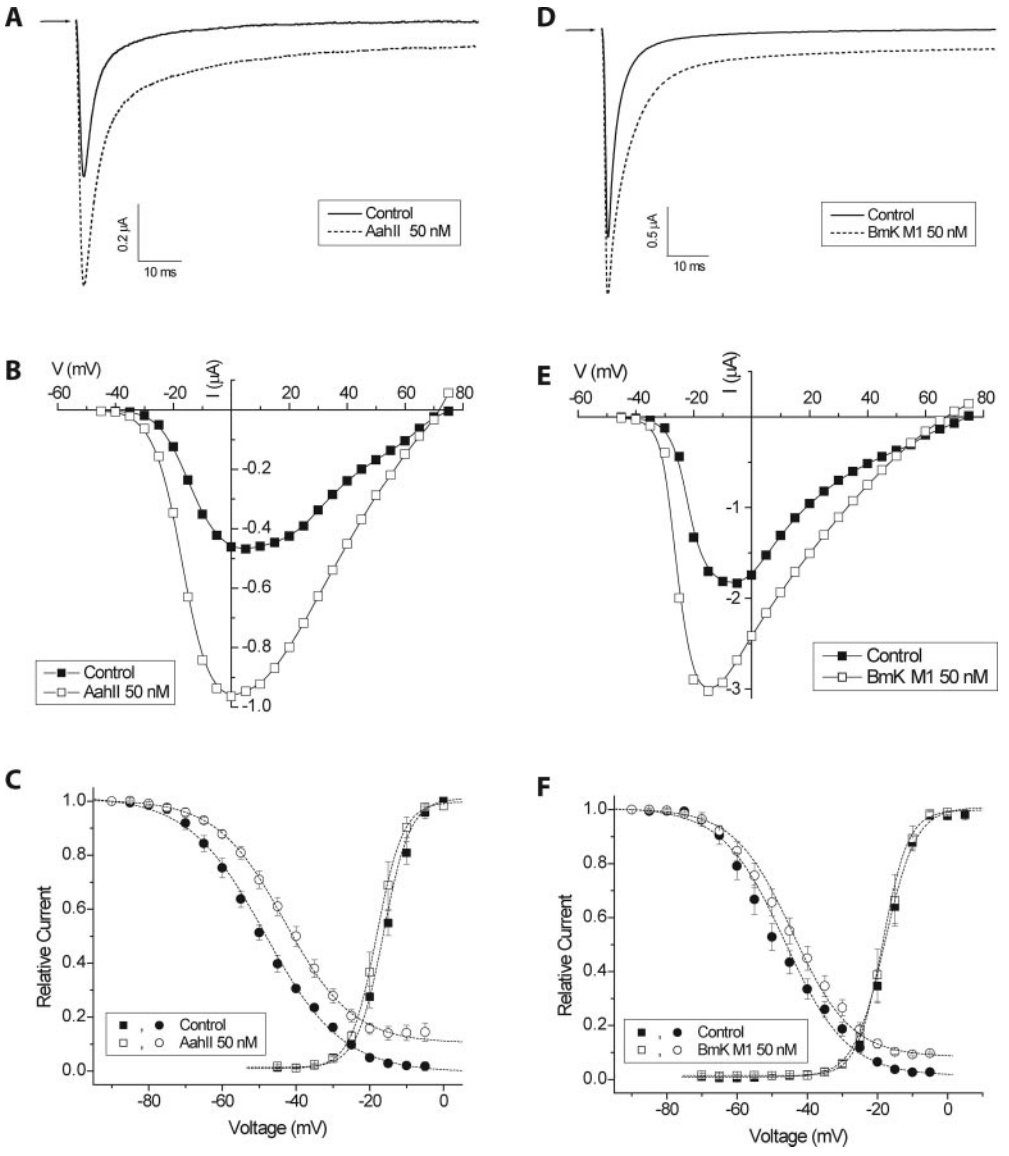

Fig. 6. Effects of AahII and BmK M1 on $Na_v1.7$. Top, representative whole-cell Na^+ currents of an oocyte expressing $Na_v1.7$ channels, in response to a 100-ms voltage pulse to V_{max} (0 mV). Solid lines represent control currents, dashed lines represent the current in the presence of 50 nM AahII (A) and BmK M1 (D). Arrow indicates zero current. B and E show the corresponding current-voltage relationships in control conditions (■) and in the presence of toxin (□), recorded from the same oocyte as in A and D, respectively. C and F depict the activation and steady-state inactivation curves in control conditions (filled symbols) and in the presence of toxin (open symbols). Activation curves (squares) were derived from the same family of currents used for the current-voltage relationships. Steady-state inactivation curves (circles) were determined using conditioning pulses to voltages between −90 and 0 mV and a standard test pulse to 0 mV. Test currents were normalized and plotted against the conditioning voltage. Each data point is an average of four experiments. The dashed lines are Boltzmann fits. See Table 2 and 3 for $V_{1/2}$ values and slope factors.

$Na_v1.8$. We showed that they had different sensitivities to OD1. $Na_v1.7$ was 250-fold more sensitive to OD1 than to $Na_v1.3$, whereas $Na_v1.8$ was not affected at the tested concentrations. The EC_{50} value for modulation of $Na_v1.7$ is 4.5 nM, demonstrating that OD1 is one of the most potent ligands for $Na_v1.7$ described at present.

OD1 was recently characterized as an α-like toxin. Jalali et al. showed that the inactivation process of the insect VGSC, para, was severely hampered by 200 nM OD1. However, the mammalian VGSCs $Na_v1.2$ and $Na_v1.5$ were not at all affected by concentrations up to 1 μM (Jalali et al., 2005). Unlike OD1, the other toxins known as $Na_v1.7$ modulators do not exhibit this selectivity pattern. Heinemann and coworkers (Chen and Heinemann, 2001; Chen et al., 2002) demonstrated that the scorpion toxin Lqh-3 (Fig. 1) from *L. quinquestriatus hebraeus* impairs fast inactivation of $Na_v1.7$ with an EC_{50} value of 14 nM but that $Na_v1.5$ is even more sensitive (EC_{50} 2.5 nM). Lqh-2 (Fig. 1) was shown to restrain the fast inactivation process of $Na_v1.7$ with an EC_{50} value of 32 nM, whereas the values for $Na_v1.2$ and $Na_v1.5$ were 1.8 and 12 nM, respectively. In addition, the tarantula peptides ProTx-I and ProTx-II inhibit the activation of $Na_v1.7$ as well as other VGSCs ($Na_v1.2$, $Na_v1.5$, and $Na_v1.8$) with IC_{50} values below 100 nM (Middleton et al., 2002).

This work demonstrates that OD1 affects the gating of $Na_v1.7$ at low nanomolar concentrations, resulting in 1) an impairment of fast inactivation, 2) a marked increase in peak Na^+ influx, and 3) a substantial persistent Na^+ current, compared with control conditions. This noninactivating current is reflected by the failure of steady state availability to reach zero, even at positive potentials. As a consequence, in the presence of OD1, channels will conduct much more inward Na^+ current than in the absence of the toxin. To examine whether these multiple effects are typical for OD1, it was compared with a classic α-toxin, AahII (Fig. 1) from *A. australis* Hector (Rochat et al., 1972), and a classic α-like toxin, BmK M1 (Fig. 1) from *B. martensii* Karsch (Ji et al., 1996). Our data show that these multiple effects on $Na_v1.7$ are not exceptional for OD1, because the effects of AahII and BmK M1 were similar to those of OD1. However, in contrast to those toxins, OD1 is unique in its selectivity for $Na_v1.7$ over $Na_v1.2$, $Na_v1.3$, and $Na_v1.5$. Unlike OD1, AahII is a potent modulator of rat brain sodium channels, and it was shown that 0.5 nM concentrations of this toxin have dramatic effects on the inactivation process (Gordon et al., 1996). Our data demonstrate that 50 nM AahII severely hampers fast inactivation of $Na_v1.3$. In addition, BmK M1 impairs the inactivation of $Na_v1.5$ channels with an EC_{50} value of 195 nM (native toxin) (Goudet et al., 2001) or 500 nM (recombinant BmK M1) (Liu et al., 2005).

Some scorpion neurotoxins show specificity for insect or mammalian VGSCs and others are able to discriminate between VGSC subtypes. This selectivity is attributed to differences in active sites on the toxins and to variations in receptor binding sites on distinct VGSCs. All scorpion α-toxins bind to receptor site 3, which involves the extracellular loop between segments S3 and S4 of domain IV of the VGSC (Rogers et al., 1996) and the extracellular loops S5–S6 of domain I and IV (Tejedor and Catterall, 1988; Thomson and Catterall, 1989). Mutagenesis within the external linker S3–S4 in domain IV of rat $Na_v1.2$ identified a negatively charged residue, Glu1613 as a major determinant that affects the binding (Rogers et al., 1996). The authors propose that nonacidic residues in the extracellular loops S5–S6 of domain I and IV may contribute to α-scorpion toxin binding by providing unique determinants that are involved in the interactions between the toxin and the channel. To understand the pharmacological selectivity pattern of OD1, we compared the amino acid sequences of receptor site 3 of $Na_v1.7$ with $Na_v1.2$, $Na_v1.3$, $Na_v1.5$, and the insect sodium channel para. Aligning the sequences, using the ClustalW algorithm, revealed no striking differences in S5–S6 of domain I and S3–S4 of domain IV. In S5–S6 of domain IV, $Na_v1.7$ and para have an asparagine at position 1674,

TABLE 2
Effects of AahII on fast activation and inactivation parameters for $Na_v1.7$ and $Na_v1.3$

	Activation			Inactivation		
	$V_{1/2}$	Slope	n	$V_{1/2}$	Slope	n
	mV			mV		
$Na_v1.7$						
Control	−16.3 ± 0.5	3.6 ± 0.3	4	−48.4 ± 0.5*	10.4 ± 0.4	4
AahII 50 nM	−18.1 ± 0.5	4.1 ± 0.2	4	−43.1 ± 0.4*	9.2 ± 0.2	4
$Na_v1.3$						
Control	−19.6 ± 0.8*	4.6 ± 0.4	4	−31.6 ± 0.2	7.5 ± 0.1	4
AahII 50 nM	−28.2 ± 0.9*	3.2 ± 0.5	4	−32.9 ± 1.6	8.2 ± 0.6	4

* $P < 0.05$

TABLE 3
Effects of BmK M1 on fast activation and inactivation parameters for $Na_v1.7$ and $Na_v1.3$

	Activation			Inactivation		
	$V_{1/2}$	Slope	n	$V_{1/2}$	Slope	n
	mV			mV		
$Na_v1.7$						
Control	−17.9 ± 0.7	4.4 ± 0.2	4	−46.4 ± 0.8*	8.9 ± 0.5	4
BmK M1 50 nM	−18.5 ± 0.3	3.6 ± 0.1	4	−44.1 ± 0.7*	8.3 ± 0.3	4
$Na_v1.3$						
Control	−15.7 ± 0.3	3.7 ± 0.2	4	−31.2 ± 0.2	7.4 ± 0.2	4
BmK M1 50 nM	−14.4 ± 0.3	4.4 ± 0.3	4	−29.4 ± 0.1	7.8 ± 0.1	4

* $P < 0.05$

whereas $Na_v1.2$, $Na_v1.3$, and $Na_v1.5$ have an aspartic acid. This asparagine probably contributes to the sensitivity of $Na_v1.7$ and para to OD1. Finally, it is noteworthy that $Na_v1.8$, which seems to be resistant to all tested scorpion α-toxins, has an uncharged hydrophobic amino acid, alanine, at the corresponding position of Glu1613 in $Na_v1.2$ in the S3–S4 extracellular loop of domain IV. This might explain the resistance of $Na_v1.8$ to scorpion α-toxins.

VGSCs open when the membrane potential is depolarized and close on repolarization, but also on continuous depolarization by a process termed inactivation, which leaves the channel refractory (i.e., unable to open again for a period of time). For the process of fast inactivation, this time is of the millisecond range but it can last much longer (up to seconds) in a different slow type of inactivation. Fast inactivation is highly vulnerable and is known to be affected by many agents, including toxins (Ulbricht, 2005). Our data show that on the one hand, OD1 impairs the process of fast inactivation of $Na_v1.7$; on the other hand, it accelerates the recovery from fast inactivation. This is in accordance with the work of Hank and coworkers, who demonstrated that the site 3 sea anemone toxin Anthopleurin B prolongs the macroscopic inactiva-

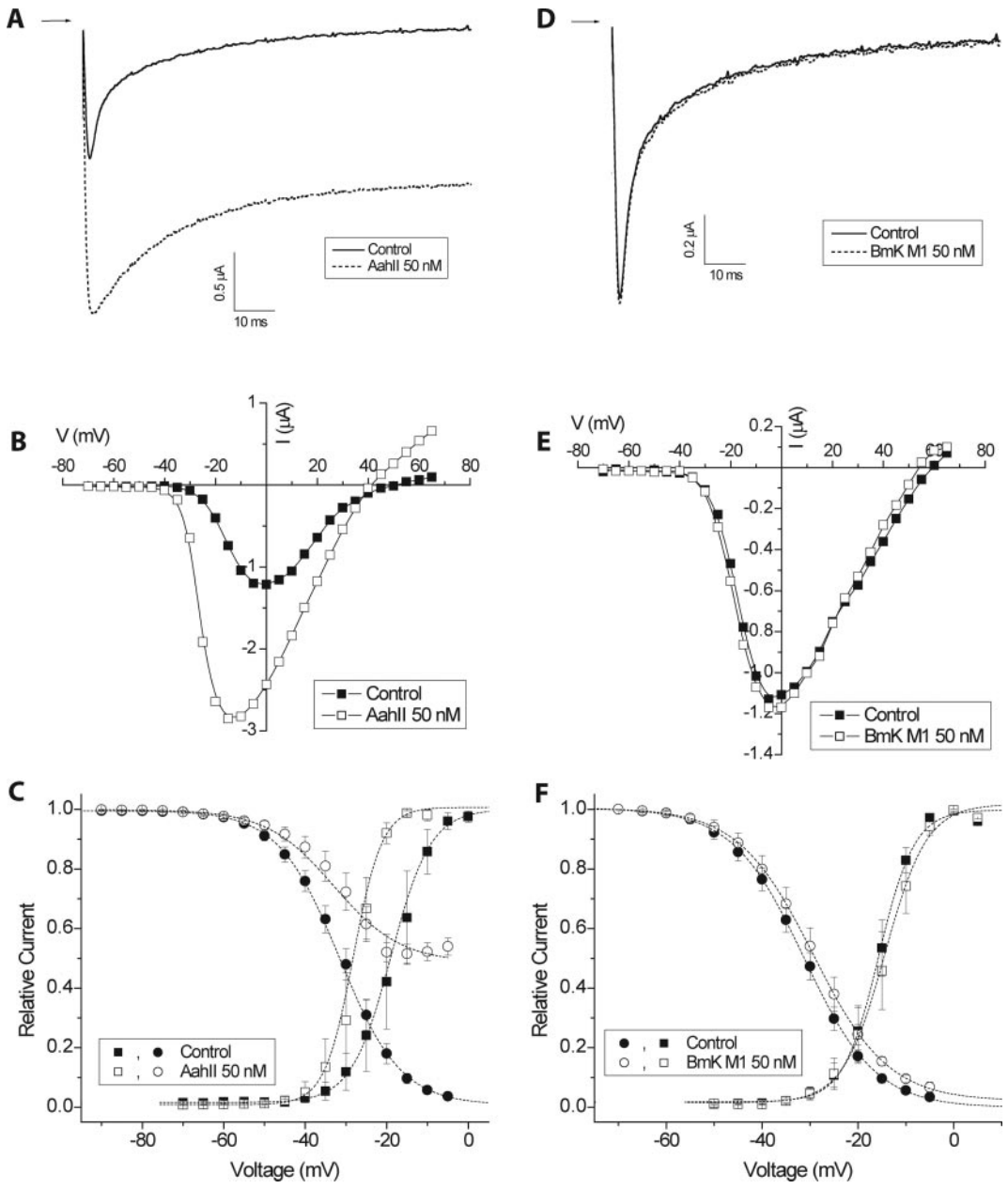

Fig. 7. Effects of AahII and BmK M1 on $Na_v1.3$. Top, representative whole-cell Na^+ currents of an oocyte expressing $Na_v1.3$ channels, in response to a 100-ms voltage pulse to V_{max} (−5 mV). Solid lines represent control currents, dashed lines represent the current in the presence of 50 nM AahII (A) and BmK M1 (D). Arrow indicates zero current. B and E show the corresponding current-voltage relationships in control conditions (■) and in the presence of toxin (□), recorded from the same oocyte as in A and D, respectively. C and F depict the activation and steady-state inactivation curves in control conditions (filled symbols) and in the presence of toxin (open symbols). Activation curves (squares) were derived from the same family of currents used for the current-voltage relationships. Steady-state inactivation curves (circles) were determined using conditioning pulses to voltages between −90 and −5 mV and a standard test pulse to −5 mV. Test currents were normalized and plotted against the conditioning voltage. Each data point is an average of four experiments. The dashed lines are Boltzmann fits. See Tables 2 and 3 for $V_{1/2}$ values and slope factors.

tion and increases the rate of whole-cell recovery of cardiac and neuronal VGSCs (Benzinger et al., 1997). They propose that the noninactivating current in the presence of toxin arises from an O ⇆ I equilibrium that partially favors the open state but that the overall rate of I → O recovery is still not sufficiently large to cause appreciable numbers of channels to recover through the open state during repolarization. Nonetheless, toxin treatment does augment recovery from inactivation. The authors suggest that both of these observations can be rationalized under the assumption that the toxin destabilizes the terminal inactivated state of the channel. Open-state inactivation is slowed, producing the well-known prolongation of macroscopic inactivation and increase in mean open time. This slowing, combined with a possible augmentation of the open-state recovery rate I → O, produces the observed plateau current. Finally, destabilization of the final inactivated state enhances the recovery from closed state inactivation (Benzinger et al., 1997). We assume the effects of OD1 on $Na_v1.7$ could be explained in a similar way. The increase in peak current observed in the presence of OD1 would then be compatible with an enhanced recovery from closed-state inactivation.

The VGSC $Na_v1.7$ has been implicated in several pathophysiological conditions, as acute inflammatory pain (Nassar et al., 2004), erythermalgia (Dib-Hajj et al., 2005; Drenth et al., 2005; Michiels et al., 2005), and prostate cancer (Diss et al., 2005). Mainly because of its role in pain, $Na_v1.7$ has become a interesting therapeutic target. At first one would logically think about ion channel blockers, but examination of certain sodium channelopathies suggests that other ways to inhibit the propagation of action potential trains in neurons may exist. Mutations in VGSC genes have been identified as the cause of epilepsy, periodic paralysis, muscle stiffness (myotonia), or cardiac arrhythmia. For the majority of these, the mutations produce mis-sense substitutions that result in functional channels with subtle changes in the voltage dependence of channel opening and closing (gating) (Cannon, 2002). Extensively studied examples of sodium channelopathies are the autosomal-dominantly inherited forms of myotonia and periodic paralysis. Missense mutations in *SCN4A*, the Na^+ channel α subunit of skeletal muscle, predominantly cause gain-of-function defects in which inactivation is partially disrupted or, in a few cases, activation is enhanced. The end result is that mutant channels conduct more inward Na^+ current than wild-type ones. It is noteworthy that the aberrant inward current can result in pathologically enhanced excitability (small persistent Na^+ currents 1–2% of the peak cause bursts of repetitive muscle fiber discharges producing sustained myotonic stiffness), whereas slightly more severe defects of inactivation (>3%) induce a loss of muscle excitability that manifests as flaccid weakness as a result of prolonged depolarization-induced reduction in Na^+ channel availability (Cannon, 2000). We think this last situation might be comparable with the modulation of $Na_v1.7$ by OD1.

In correlation with proinflammatory, hyperalgesic agents such as serotonin, prostaglandin E_2 and adenosine, which cause abnormal bursting activity in primary sensory neurons, OD1 causes a dose-dependent increase in the amplitude of Na^+ currents, accompanied by a leftward shift in the voltage-dependence of activation (Gold et al., 1996). However, in sharp contrast to the aforementioned hyperalgesic agents, OD1 impairs the fast inactivation process and results in an incomplete inactivation in steady-state conditions. We presume that the persistent inward Na^+ current may lead to a sustained depolarization of the cell membrane in vivo. Therefore, the remaining $Na_v1.7$ channels that were not affected by OD1 would be trapped in the inactivated state, resulting in the loss of electrical excitability of nociceptor neurons. A similar mechanism was proposed to explain feeling of numbness described after contact of skin with the VGSC modulator batrachotoxin (Bosmans et al., 2004).

In conclusion, the present study shows that the scorpion toxin OD1 is a potent modulator of $Na_v1.7$. Low nanomolar concentrations of this toxin impair the steady-state fast inactivation process, enhance the recovery from fast inactivation, increase the peak Na^+ current, and give rise to a substantial persistent Na^+ current. At these concentrations, other mammalian VGSCs ($Na_v1.2$, $Na_v1.3$, $Na_v1.5$, and $Na_v1.8$) were not affected.

Acknowledgments

We thank the following persons: S. C. Cannon (University of Texas Southwestern Medical Center, Dallas, TX) for sharing hβ1 subunit, A. L. Goldin (University of California, Irvine, CA) for sharing $Na_v1.3$, S. H. Heinemann (Friedrich-Schiller-Universität Jena, Germany) for sharing the rβ_1 subunit, M.-F. Martin-Eauclaire (Centre National de la Recherche Scientifique, Université de la Méditerranée, Marseille, France) for AahII, and D.-C. Wang (Center for Structural and Molecular Biology, Institute of Biophysics, Beijing, People's Republic of China) for BmK M1. We are grateful to Roche (Palo Alto, CA) for sharing rNav1.7 and hNav1.8. We thank L. Schoofs and E. Clynen (University of Leuven, Belgium) for mass and sequence determination of OD1 and Kristof Prinsen for help with the electrophysiological experiments.

References

Benzinger GR, Drum CL, Chen LQ, Kallen RG, Hanck DA, and Hanck D (1997) Differences in the binding sites of two site-3 sodium channel toxins. *Pflueg Arch Eur J Physiol* **434:**742–749.

Bosmans F, Maertens C, Verdonck F, and Tytgat J (2004) The poison dart frog's batrachotoxin modulates Nav1.8. *FEBS Lett* **577:**245–248.

Cannon SC (2002) Sodium channel gating: no margin for error. *Neuron* **34:**853–854.

Cannon SC (2000) Spectrum of sodium channel disturbances in the nondystrophic myotonias and periodic paralyses. *Kidney Int* **57:**772–779.

Cao ZY, Mi ZM, Cheng GF, Shen WQ, Xiao X, Liu XM, Liang XT, and Yu DQ (2004) Purification and characterization of a new peptide with analgesic effect from the scorpion *Buthus martensi* Karch. *J Pept Res* **64:**33–41.

Catterall WA, Goldin AL, and Waxman SG (2005) International Union of Pharmacology. XLVII. Nomenclature and structure-function relationships of voltage-gated sodium channels. *Pharmacol Rev* **57:**397–409.

Chen B and Ji Y (2002) Antihyperalgesia effect of BmK AS, a scorpion toxin, in rat by intraplantar injection. *Brain Res* **952:**322–326.

Chen H, Gordon D, and Heinemann SH (2000) Modulation of cloned skeletal muscle sodium channels by the scorpion toxins Lqh II, Lqh III and Lqh alphaIT. *Pflueg Arch Eur J Physiol* **439:**423–432.

Chen H and Heinemann SH (2001) Interaction of scorpion alpha-toxins with cardiac sodium channels: binding properties and enhancement of slow inactivation. *J Gen Physiol* **117:**505–518.

Chen H, Lu S, Leipold E, Gordon D, Hansel A, and Heinemann SH (2002) Differential sensitivity of sodium channels from the central and peripheral nervous system to the scorpion toxins Lqh-2 and Lqh-3. *Eur J Neurosci* **16:**767–770.

Chevrier P, Vijayaragavan K, and Chahine M (2004) Differential modulation of Nav1.7 and Nav1.8 peripheral nerve sodium channels by the local anesthetic lidocaine. *Br J Pharmacol* **142:**576–584.

Dib-Hajj SD, Rush AM, Cummins TR, Hisama FM, Novella S, Tyrrell L, Marshall L, and Waxman SG (2005) Gain-of-function mutation in Nav1.7 in familial erythromelalgia induces bursting of sensory neurons. *Brain* **128:**1847–1854.

Diss JK, Stewart D, Pani F, Foster CS, Walker MM, Patel A, and Djamgoz MB (2005) A potential novel marker for human prostate cancer: voltage-gated sodium channel expression in vivo. *Prostate Cancer Prostatic Dis* **8:**266–273.

Drenth JP, te Morsche RH, Guillet G, Taieb A, Kirby RL, and Jansen JB (2005) SCN9A mutations define primary erythermalgia as a neuropathic disorder of voltage gated sodium channels. *J Investig Dermatol* **124:**1333–1338.

Gold MS, Reichling DB, Shuster MJ, and Levine JD (1996) Hyperalgesic agents increase a tetrodotoxin-resistant Na^+ current in nociceptors. *Proc Natl Acad Sci USA* **93:**1108–1112.

Gordon D, Martin-Eauclaire MF, Cestele S, Kopeyan C, Carlier E, Khalifa RB,

Pelhate M, and Rochat H (1996) Scorpion toxins affecting sodium current inactivation bind to distinct homologous receptor sites on rat brain and insect sodium channels. *J Biol Chem* **271:**8034–8045.
Goudet C, Chi CW, and Tytgat J (2002) An overview of toxins and genes from the venom of the Asian scorpion *Buthus martensi* Karsch. *Toxicon* **40:**1239–1258.
Goudet C, Huys I, Clynen E, Schoofs L, Wang DC, Waelkens E, and Tytgat J (2001) Electrophysiological characterization of BmK M1, an alpha-like toxin from *Buthus martensi* Karsch venom. *FEBS Lett* **495:**61–65.
Guan R, Wang CG, Wang M, and Wang DC (2001a) A depressant insect toxin with a novel analgesic effect from scorpion *Buthus martensii* Karsch. *Biochim Biophys Acta* **1549:**9–18.
Guan RJ, Liu XQ, Liu B, Wang M, and Wang DC (2000) Crystallization and preliminary X-ray analyses of insect neurotoxins with analgesic effect from the scorpion *Buthus martensii* Karsch. *Acta Crystallogr Sect D* **56 (Pt 8):**1012–1014.
Guan RJ, Wang M, Wang D, and Wang DC (2001b) A new insect neurotoxin AngP1 with analgesic effect from the scorpion *Buthus martensii* Karsch: purification and characterization. *J Pept Res* **58:**27–35.
Jalali A, Bosmans F, Amininasab M, Clynen E, Cuypers E, Zaremirakabadi A, Sarbolouki MN, Schoofs L, Vatanpour H, and Tytgat J (2005) OD1, the first toxin isolated from the venom of the scorpion *Odonthobuthus doriae* active on voltage-gated Na^+ channels. *FEBS Lett* **579:**4181–4186.
Ji YH, Mansuelle P, Terakawa S, Kopeyan C, Yanaihara N, Hsu K, and Rochat H (1996) Two neurotoxins (BmK I and BmK II) from the venom of the scorpion *Buthus martensi* Karsch: purification, amino acid sequences and assessment of specific activity. *Toxicon* **34:**987–1001.
Liu LH, Bosmans F, Maertens C, Zhu RH, Wang DC, and Tytgat J (2005) Molecular basis of the mammalian potency of the scorpion alpha-like toxin, BmK M1. *FASEB J* **19:**594–596.
Liu YF, Ma RL, Wang SL, Duan ZY, Zhang JH, Wu LJ, and Wu CF (2003) Expression of an antitumor-analgesic peptide from the venom of Chinese scorpion *Buthus martensii* Karsch in *Escherichia coli*. *Protein Expr Purif* **27:**253–258.
McNulty MM and Hanck D (2004) A state-dependent mibefradil block of Na^+ channels. *Mol Pharmacol* **66:**1652–1661.
Meisler MH and Kearney J (2005) A sodium channel mutations in epilepsy and other neurological disorders. *J Clin Investig* **115:**2010–2017.
Michiels JJ, te Morsche RH, Jansen JB, and Drenth JP (2005) Autosomal dominant erythermalgia associated with a novel mutation in the voltage-gated sodium channel {alpha} subunit Nav1.7. *Arch Neurol* **62:**1587–1590.
Middleton RE, Warren VA, Kraus RL, Hwang JC, Liu CJ, Dai G, Brochu RM, Kohler MG, Gao YD, Garsky VM, et al. (2002) Two tarantula peptides inhibit activation of multiple sodium channels. *Biochemistry* **41:**14734–14747.
Nassar MA, Stirling LC, Forlani G, Baker MD, Matthews EA, Dickenson AH, and Wood JN (2004) Nociceptor-specific gene deletion reveals a major role for Nav1.7 (PN1) in acute and inflammatory pain. *Proc Natl Acad Sci USA* **101:**12706–12711.
Possani LD, Becerril B, Delepierre M, and Tytgat J (1999) Scorpion toxins specific for Na^+-channels. *Eur J Biochem* **264:**287–300.
Rochat H, Rochat C, Sampieri F, Miranda F, and Lissitzky S (1972) The amino-acid sequence of neurotoxin II of *Androctonus australis* hector. *Eur J Biochem* **28:**381–388.
Rodriguez de la Vega RC and Possani LD (2005) Overview of scorpion toxins specific for Na^+ channels and related peptides: biodiversity, structure-function relationships and evolution. *Toxicon* **46:**831–844.
Rogers JC, Qu Y, Tanada TN, Scheuer T, and Catterall WA (1996) Molecular determinants of high affinity binding of α-scorpion toxin and sea anemone toxin in the S3–S4 extracellular loop in domain IV of the Na^+ channel α subunit. *J Biol Chem* **271:**15950–15962.
Tejedor FJ and Catterall WA (1988) Site of covalent attachment of α-toxin derivatives in domain I of the sodium channel α subunit. *Proc Natl Acad Sci USA* **85:**8742–8746.
Thomson WJ and Catterall WA (1989) Localization of the receptor site for α-scorpion toxins by antibody mapping: implications for sodium channel topology. *Proc Natl Acad Sci USA* **86:**10161–10165.
Tytgat J, Maertens C, and Daenens P (1997) Effect of fluoxetine on a neuronal, voltage-dependent potassium channel (Kv1.1). *Br J Pharmacol* **122:**1417–1424.
Ulbricht W (2005) Sodium channel inactivation: molecular determinants and modulation. *Physiol Rev* **85:**1271–1301.
Wang CY, Tan ZY, Chen B, Zhao ZQ, and Ji YH (2000) Antihyperalgesia effect of BmK IT2, a depressant insect-selective scorpion toxin in rat by peripheral administration. *Brain Res Bull* **53:**335–338.
Wang SY and Wang GK (2003) Voltage-gated sodium channels as primary targets of diverse lipid-soluble neurotoxins. *Cell Signal* **15:**151–159.
Waxman SG and Dib-Hajj S (2005) Erythermalgia: molecular basis for an inherited pain syndrome. *Trends Mol Med* **11:**555–562.
Wood JN, Boorman JP, Okuse K, and Baker MD (2004) Voltage-gated sodium channels and pain Pathways. *J Neurobiol* **61:**55–71.
Xiong YM, Lan ZD, Wang M, Liu B, Liu XQ, Fei H, Xu LG, Xia QC, Wang CG, Wang DC, et al. (1999) Molecular characterization of a new excitatory insect neurotoxin with an analgesic effect on mice from the scorpion *Buthus martensi* Karsch. *Toxicon* **37:**1165–1180.
Yeomans DC, Levinson SR, Peters MC, Koszowski AG, Tzabazis AZ, Gilly WF, and Wilson SP (2005) Decrease in inflammatory hyperalgesia by herpes vector-mediated knockdown of Nav1.7 sodium channels in primary afferents. *Hum Gene Ther* **16:**271–277.

Address correspondence to: J. Tytgat, Laboratory of Toxicology, University of Leuven, Onderwijs and Navorsing II, Herestraat 49 – Box 922, B-3000 Leuven, Belgium. E-mail: Jan.Tytgat@pharm.kuleuven.be